



This is a repository copy of *Spin-echo small-angle neutron scattering (SESANS) studies of diblock copolymer nanoparticles*.

White Rose Research Online URL for this paper:
<http://eprints.whiterose.ac.uk/140739/>

Version: Accepted Version

Article:

Smith, G.N. orcid.org/0000-0002-0074-5657, Cunningham, V.J., Canning, S.L. et al. (4 more authors) (2019) Spin-echo small-angle neutron scattering (SESANS) studies of diblock copolymer nanoparticles. *Soft Matter*, 15 (1). pp. 17-21. ISSN 1744-683X

<https://doi.org/10.1039/c8sm01425f>

© 2019 The Royal Society of Chemistry. This is an author produced version of a paper subsequently published in *Soft Matter*. Uploaded in accordance with the publisher's self-archiving policy.

Reuse

Items deposited in White Rose Research Online are protected by copyright, with all rights reserved unless indicated otherwise. They may be downloaded and/or printed for private study, or other acts as permitted by national copyright laws. The publisher or other rights holders may allow further reproduction and re-use of the full text version. This is indicated by the licence information on the White Rose Research Online record for the item.

Takedown

If you consider content in White Rose Research Online to be in breach of UK law, please notify us by emailing eprints@whiterose.ac.uk including the URL of the record and the reason for the withdrawal request.



eprints@whiterose.ac.uk
<https://eprints.whiterose.ac.uk/>

Cite this: DOI: 10.1039/xxxxxxxxxx

Spin-echo small-angle neutron scattering (SESANS) studies of diblock copolymer nanoparticles[†]

Gregory N. Smith,^{*a‡} Victoria J. Cunningham,^{a¶} Sarah L. Canning,^{a§} Matthew J. Derry,^a J. F. K. Cooper,^b A. L. Washington,^b and Steven P. Armes^a

Received Date

Accepted Date

DOI: 10.1039/xxxxxxxxxx

www.rsc.org/journalname

Poly(glycerol monomethacrylate)–poly(benzyl methacrylate) (PGMA–PBzMA) diblock copolymer nanoparticles were synthesized via polymerization-induced self-assembly (PISA) using reversible addition–fragmentation chain transfer (RAFT) aqueous emulsion polymerization in D₂O. Such PISA syntheses produce sterically-stabilized nanoparticles *in situ* and can be performed at relatively high copolymer concentrations (up to 50 wt. %). This PGMA–PBzMA formulation is known to form only spherical nanoparticles in water using aqueous emulsion polymerization (*Macromolecules*, 2014, 47, 5613–5623), which makes it an ideal model system for exploring new characterization methods. The polymer micelles were characterized using small-angle X-ray scattering (SAXS) and a recently developed form of neutron scattering, spin-echo small-angle neutron scattering (SESANS). As far as we are aware, this is the first report of a study of polymer micelles by SESANS, and the data agree well with reciprocal space scattering. Using this technique enables characterization of the concentrated, as synthesized dispersions directly without dilution, and this provides a method to study self-assembled polymer systems that have concentration dependent morphologies in the future, while still maintaining the advantages of

scattering techniques.

Polymerization-induced self-assembly (PISA) enables the convenient synthesis of a wide range of diblock copolymer nano-objects directly in water, or other solvents, using either RAFT aqueous dispersion polymerization or RAFT aqueous emulsion polymerization.¹ Dispersion polymerization requires a monomer that is miscible with the solvent but produces a polymer that is insoluble in the solvent. In water, there are relatively few monomers that meet these requirements. One such vinyl monomer is 2-hydroxypropyl methacrylate (HPMA), which has been well studied in the context of PISA.² In contrast, most vinyl monomers exhibit relatively low aqueous solubility (less than 20 g L⁻¹) and hence are well suited for aqueous emulsion polymerization. In this case, the monomer only requires sufficient solubility to facilitate mass transport between large monomer droplets and the growing polymer chains.¹ Monomers such as benzyl methacrylate meet this requirement,³ and this monomer is used as the core-forming block in the present study. Poly(glycerol monomethacrylate) (PGMA) is used as the steric stabilizer block.

The PISA protocol used to prepare the PGMA–PBzMA diblock copolymers is shown in Scheme 1. 2-Cyano-2-propyl benzodithioate (CPDB) was used as the RAFT chain transfer agent (CTA), and 4,4'-azobis(4-cyanovaleric acid) (ACVA) was selected as the radical initiator. The reaction conditions indicated in Scheme 1 are the same as those previously reported for the RAFT aqueous emulsion polymerization of BzMA.³ For the present study, this protocol was modified by preparing the nanoparticles in D₂O to obtain maximum contrast for neutron scattering experiments. To ensure that the nanoparticles were identical for both X-ray and neutron scattering experiments, D₂O was used as the solvent for both.

The diblock copolymers were characterized both in solution (using ¹H NMR spectroscopy to determine the final BzMA conversion and calculate the mean diblock composition as well as gel permeation chromatography to determine molar mass and dis-

^a University of Sheffield, Department of Chemistry, Dainton Building, Brook Hill, Sheffield, South Yorkshire, S3 7HF, United Kingdom

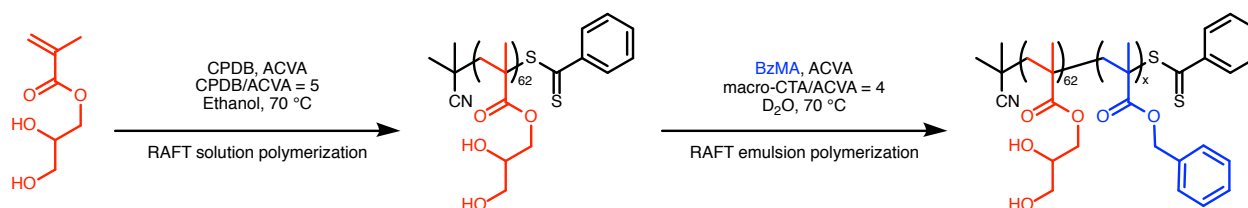
^b ISIS-STFC, Rutherford Appleton Laboratory, Chilton, Oxon OX11 0QX, United Kingdom.

[†] Electronic Supplementary Information (ESI) available. See DOI: 10.1039/b000000x/. SESANS data available from ISIS Data Journal. See DOI: 10.5286/ISIS.E.83549865. Additional data available from the Zenodo repository. See DOI: 10.5281/zenodo.1308812.

[‡] Present address: Niels Bohr Institute, University of Copenhagen, Universitetsparken 5, 2100 Copenhagen, Denmark. Email address: gregory.smith@nbi.ku.dk.

[¶] Present address: Scott Bader Company Ltd., Wollaston, NN29 7RL, United Kingdom.

[§] Present address: Fujifilm Speciality Ink Systems Ltd, Pysons Road, Broadstairs, Kent CT10 2LE, United Kingdom.



Scheme 1 Synthesis of PGMA₆₂-PBzMA_x diblock copolymer nanoparticles by (i) RAFT solution polymerization of GMA in ethanol to afford a PGMA₆₂ macromolecular CTA and (ii) RAFT aqueous emulsion polymerization of BzMA at 70 °C using the synthesized macromolecular CTA.

persity, Supporting Information Table S2) and also as sterically-stabilized nanoparticles (using dynamic light scattering to determine the hydrodynamic radius and transmission electron microscopy to determine morphology, Supporting Information Table S1 and Figure S3). Monomer conversions, determined by comparing the integrated oxymethylene signals assigned to the BzMA monomer and PBzMA polymer in a ¹H NMR spectrum recorded in dimethylformamide-*d*₇, were extremely high (> 99%) for all diblock copolymers. Molar masses (*M_n*) from gel permeation chromatography (GPC) were comparable to those determined from ¹H NMR, and the dispersities ($D_M = M_w/M_n$) were relatively low, as expected for a well-controlled RAFT polymerization. The nanoparticles also appear to be spherical, with monotonically increasing *Z*-average diameters (*d_Z*) and relatively low polydispersity indexes determined from dynamic light scattering (DLS). However, the size distributions are broader and the mean diameters are somewhat lower than data reported for comparable PGMA₅₁-PBzMA_x copolymer nanoparticles prepared by RAFT aqueous emulsion polymerization previously (Supporting Information Figure S4).³ These differences may be due to using D₂O compared to H₂O. However, the discrepancies are relatively small. Crucially for scattering analysis, these PGMA₆₂-PBzMA_x nanoparticles maintain the same spherical morphology as that observed when synthesized in H₂O.

The structural properties of these sterically-stabilized PGMA₆₂-PBzMA_x nanoparticles were studied using small-angle X-ray scattering (SAXS) and spin-echo small-angle neutron scattering (SESANS). The two give complementary detail about the polymer spheres, as previously shown for sterically-stabilized polystyrene colloids.⁴ The ability of each technique to resolve structures depends on the contrast between the blocks and the solvent and the length scale that can be accessed. X-ray scattering arises from the interaction of photons with electrons; hence SAXS is sensitive to differences in electron density between the dispersed phase and the solvent.⁵ Given the scattering angles accessible by conventional SAXS instruments, this technique enables determination of both the overall size and internal structure of the nanoparticles.⁵ On the other hand, neutron scattering arises from the interaction of neutrons with atomic nuclei; hence, high contrast can be achieved in SANS experiments by dispersing nanoparticles in isotopically-labeled solvent, as done in this study.⁶ In particular, very high contrasts can be achieved using SESANS, as multiple scattering can be trivially corrected for. Additionally, longer length scales are accessible, enabling both particle size and inter-particle interactions to be determined.⁷

Synchrotron SAXS measurements were performed on 1 wt. % dispersions of PGMA₆₂-PBzMA_x nanoparticles in D₂O at the ID02 beamline at the ESRF (Grenoble, France). Full details of the instrument configuration can be found elsewhere.⁸ Monochromatic X-ray radiation (with wavelength $\lambda = 0.995 \text{ \AA}$) was used with a sample-detector distance of 5.0042 m. This gave an accessible *Q*-range of $0.0015 \leq Q \leq 0.15 \text{ \AA}^{-1}$. *Q* is defined as the magnitude of the momentum transfer vector and depends on both λ and θ (one half of the scattering angle) ($Q = (4\pi \sin \theta)/(\lambda)$). SAXS has proved to be a very powerful technique for determining the structure of diblock copolymer nano-objects in general,^{1,9} and, more specifically, the PISA syntheses of sterically-stabilized diblock copolymer nanoparticles directly in water.¹⁰⁻¹³ Experimental SAXS data and corresponding model fits are shown in Figure 1, and *I(Q)* is essentially independent of *Q* at low-*Q*, which is consistent with the formation of spherical nanoparticles. The data have been fitted to a spherical diblock copolymer micelle model with a Gaussian distribution of core radii.¹⁴⁻¹⁶ The model depends on scattering length densities (SLD, ρ) of the blocks and solvent and the volume of each of the polymer blocks, all of which were calculated from the known physical properties of the polymers, which are fixed parameters. Further details on the model and calculation of these parameters are provided in the Supporting Information. The model also depends on the radius of the PBzMA nanoparticle core, which is directly proportional to the aggregation number, and the radius of gyration of the PGMA stabilizer, *R_g* (initially fixed to a physically reasonable estimate and then allowed to vary). The data were modeled using the Irena package for Igor Pro using a custom-written model.¹⁷

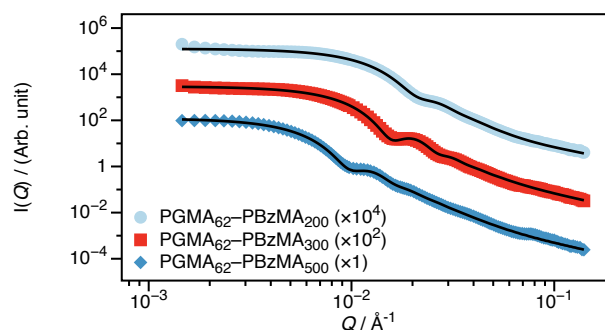


Fig. 1 SAXS data recorded 1 wt. % dispersions of PGMA₆₂-PBzMA_x nanoparticles in D₂O (the core DP, *x*, is stated in the legend). These data are consistent with the formation of spherical nanoparticles and can be well described using a spherical diblock copolymer micelle model.

Both the nanoparticle radius and the mean aggregation number of the micelles increase monotonically as the PBzMA DP is increased, as expected.¹⁸ Relatively small spheres with core diameters less than 100 nm and reasonably narrow size distributions with coefficients of variation between 0.1 and 0.2 were obtained in all cases. A summary of the best fit parameters are given in the Supporting Information (Table S6). While reciprocal space scattering is well-suited for determining the nanoparticle structure, it is generally ill-suited for characterizing interparticle interactions. This is because the necessary inclusion of the structure factor ($S(Q)$) required to model interactions complicates the data analysis, as the scattering intensity becomes the product of $S(Q)$ and the form factor ($P(Q)$). Additionally, quantification of long-range interactions requires data at extremely low- Q , which is not accessible on all instrumentation or at all facilities. Therefore, reciprocal space scattering experiments are often conducted on dilute dispersions, as is the case for this SAXS study.

As a technique, SESANS overcomes this limitation. While it lacks the short-range structural resolution offered by reciprocal space SAXS, it enables measurements of objects up to microscopic sizes, quantification of interparticle interactions in dispersions of any concentration, and high contrasts between solute and solvent to be studied from isotopic substitution without concerns over multiple scattering. Recent experiments have shown that SESANS is a powerful method for studying colloidal materials, in particular.^{4,19–24} In this study, we take advantage of these capabilities of SESANS to study PGMA₆₂–PBzMA_{*x*} nanoparticles directly as synthesized at a concentration of 30 wt. %. With the high contrast between the copolymer and solvent attainable, it should be possible to quantify the volume fraction of water (D₂O) entrapped by the PGMA-stabilizer as well as the nanoparticle size and interactions.

SESANS measurements were performed directly on all PGMA₆₂–PBzMA_{*x*} dispersions in D₂O without dilution. Measurements were performed on the Offspec beamline at the ISIS Spallation Source (Didcot, UK). The implementation of spin echo on Offspec is nonstandard, as it encodes spatial, rather than temporal information. For further technical details, see the discussion by Plomp.²⁵ The neutron spin echo length (Z) depends on the strength (B) of the magnetic field and the angle (θ) of its interface with respect to the neutron beam ($Z = (\gamma_L m B \lambda^2 L \cot \theta) / (2\pi h)$). In spin echo mode, Offspec has a usable wavelength (λ) range between 2.2 and 14 Å. The magnetic field is fixed by the spin flippers to 17.1 mT, and angles of 85° and 57° were used. Using values of the gyromagnetic ratio (γ_L), neutron mass (m), and the Planck constant (h), as well the magnetic field length ($L = 1.0$ m), the calculated spin echo lengths for a 10 Å neutron would be 263 Å and 1502 Å respectively, for these angles.

Experimental SESANS data along with model fits are shown in Figure 2. As the DP of the core-forming PBzMA block is increased from 200 to 500, the first minimum in the normalized spin-echo signal is shifted to longer spin-echo length. This is consistent with the presence of nanoparticles of increasing size. The scattering data from the nanoparticles were modeled as non-interacting hard spheres.^{26,27} This model was selected for several reasons. The SESANS signal will be dominated by the particle's

primary length scale and inter-particle structure factor, so additional model parameters would be adding extraneous degrees of freedom while providing little statistically significant detail about the sample. This is the same approach used for core-shell polymer nanoparticles studied by SESANS previously.⁴ In contrast to this previous study, where concentrated dispersions were prepared to study the interactions between colloids, we perform experiments on a colloidal dispersion that is synthesized as a concentrate. SESANS, therefore, has been shown to be a robust method to study sterically-stabilized colloids,⁴ and is therefore ideally suited to characterizing the nanoparticles that are synthesized by PISA. As can be seen in Figure 2, the data can be successfully modeled by treating the particles as homogeneous spheres. The mean diameters obtained for these sterically-stabilized nanoparticles using SAXS and SESANS compare reasonably well to the volume-weighted diameter DLS (d_V), shown in Table 1. The agreement between DLS and SAXS or SESANS is best for the technique where the particle size best matches the optimal length scale (small particles for SAXS and large particles for SESANS). For the same Q -range in a SAXS measurement, large particles will scatter less within this range than small particles, and therefore, sizes of larger particles will be less certain. In a SESANS measurement, small particles will exhibit more conventional SANS, which makes it more difficult to resolve the beam depolarization, and therefore, sizes of smaller particles will be less certain. In a DLS measurement, the certainty of the sizes of all particles should be similar. This is precisely what we observe when comparing SAXS or SESANS data to DLS data.

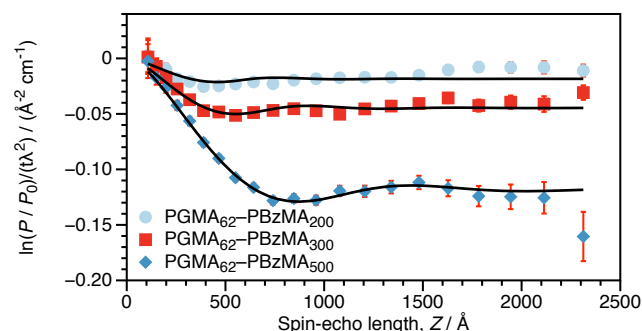


Fig. 2 Normalized spin-echo signal as a function of spin-echo length for 30 wt. % dispersions of PGMA₆₂–PBzMA_{*x*} nanoparticles in D₂O (the core DP, *x*, is stated in the legend). These data were fitted to a spherical model with hard sphere interactions with a fixed volume fraction (ϕ) and a variable scattering length density ($\Delta\rho$) between that of the sphere and the solvent.

Table 1 Mean particle diameters for PGMA₆₂–PBzMA_{*x*} nanoparticles.

	DLS d_V / nm	SAXS d / nm	SESANS d / nm
PGMA ₆₂ –PBzMA ₂₀₀	48	45	60
PGMA ₆₂ –PBzMA ₃₀₀	62	59	71
PGMA ₆₂ –PBzMA ₅₀₀	104	93	108

$$\text{SAXS: } d = 2r + 4R_g; \text{ SESANS: } d = 2r$$

From the fits to the SESANS data (d and $\Delta\rho$), it is possible to

determine the composition of the spheres. The SLD (ρ_t) of a multicomponent particle is a volume fraction (ϕ) weighted sum of the SLDs of the individual components ($\rho_t = \sum_i \phi_i \rho_i$). For these sterically-stabilized nanoparticles, the three components are the PGMA chains in the shell (ρ_s and ϕ_s), the solvating D₂O in the shell (ρ_m and ϕ_m), and the PBzMA core (ρ_c and ϕ_c). The volume fractions of the stabilizer and core for a non-solvated nanoparticle are known from the diblock composition, and the SLDs for all three pure components are also known. Thus, it is possible to calculate the ϕ_m that would be required to give the experimental ρ_t . These ρ_m values are shown in Table 2 for the three PGMA₆₂-PBzMA_x nanoparticles studied. The corresponding ϕ_m values calculated from the SAXS fitting (assuming that the stabilizer thickness is $2R_g$) are shown for comparison. These two methods compare favorably, although the best agreement is for the largest sphere where SESANS fitting is more reliable, as discussed above. Using a similar approach, the mean aggregation numbers (n_{agg}) for these nanoparticles can be determined. In the case of the SAXS data, this parameter is determined by dividing the nanoparticle core volume by the molecular volume of a single PBzMA chain. For the SESANS measurements, the fraction of the sphere that is occupied by polymer and not D₂O is determined by scaling the total sphere volume by $(1 - \phi_m)$ and dividing by the volume of the entire diblock chain. As shown in Table 2, the n_{agg} values calculated from these two approaches are gratifyingly similar. Although there are discrepancies, the two techniques require different approaches to calculating structural parameters (from the geometry for SAXS and from the contrast for SESANS), which can explain this.

Table 2 Volume fraction occupied by the D₂O solvent (ϕ_m) and mean aggregation number (n_{agg}) for PGMA₆₂-PBzMA_x nanoparticles.

	ϕ_m		n_{agg}	
	SESANS	SAXS	SESANS	SAXS
PGMA ₆₂ -PBzMA ₂₀₀	0.58	0.26	1452	1017
PGMA ₆₂ -PBzMA ₃₀₀	0.31	0.19	2463	1863
PGMA ₆₂ -PBzMA ₅₀₀	0.17	0.11	7513	5163

The advantage of using SESANS to study these PGMA₆₂-PBzMA_x nanoparticles is that no *a priori* assumptions are required, and all structural information is a consequence of the large isotopic contrast between the copolymer and the solvent. The reasonable agreement found between structural properties calculated from fitting reciprocal space SAXS data and real space SESANS data promises wider application of this new form of neutron scattering to diblock copolymer nano-objects.

Clearly, SESANS is a useful and informative technique for characterizing concentrated dispersions of relatively large nanoparticles. The results in this study show that using SESANS makes it straightforward to determine the properties of model polymer nanoparticles, providing complementary information to other forms of scattering. The ability to study concentrated dispersions is advantageous for PISA, in particular, as it is known that the concentration of nano-objects can impact the morphology that are formed even for equivalent diblock copolymers.^{2,28} The ability to study such dispersions directly, therefore, is appealing, particularly in cases where dilution results in morphological reorganiza-

tion. As advances continue to be made in both spin-echo scattering instrumentation and data analysis, we expect that SESANS will become an important tool for studying dispersions of diblock copolymer nano-objects in the future.

Conflicts of interest

There are no conflicts of interest to declare.

Acknowledgements

GNS and SPA acknowledge the ERC (PISA 320372) and EPSRC (EP/J007846) for funding. The ESRF and ISIS (experiment RB1610048) are acknowledged for allocation of beamtime and the UK Science and Technology Facilities Council for funding travel. The personnel of the ID02 beamline and Mr. T. J. Neal, Miss D. Beattie, and Mr. E. J. Cornel are acknowledged for assistance with SAXS measurements. This work benefited from the use of the SasView application, originally developed under NSF Award DMR-0520547. SasView also contains code developed with funding from the EU Horizon 2020 programme under the SINE2020 project Grant No 654000.

References

- S. L. Canning, G. N. Smith and S. P. Armes, *Macromolecules*, 2016, **49**, 1985–2001.
- N. J. Warren and S. P. Armes, *J. Am. Chem. Soc.*, 2014, **136**, 10174–10185.
- V. J. Cunningham, A. M. Alswieleh, K. L. Thompson, M. Williams, G. J. Leggett, S. P. Armes and O. M. Musa, *Macromolecules*, 2014, **47**, 5613–5623.
- K. van Gruijthuijsen, W. G. Bouwman, P. Schurtenberger and A. Stradner, *Europhys. Lett.*, 2014, **106**, 28002.
- B. R. Pauw, *J. Phys.: Condens. Matter*, 2013, **25**, 383201.
- M. J. Hollamby, *Phys. Chem. Chem. Phys.*, 2013, **15**, 10566–10579.
- M. T. Rekveldt, *Nucl. Instrum. Methods Phys. Res. B: Beam Interact. Mater. Atoms*, 1996, **114**, 366–370.
- R. Deng, M. J. Derry, C. J. Mable, Y. Ning and S. P. Armes, *J. Am. Chem. Soc.*, 2017, **139**, 7616–7623.
- J. S. Pedersen and C. Svaneborg, *Curr. Opin. Colloid Interface Sci.*, 2002, **7**, 158–166.
- A. Blanz, R. Verber, O. O. Mykhaylyk, A. J. Ryan, J. Z. Heath, C. W. I. Douglas and S. P. Armes, *J. Am. Chem. Soc.*, 2012, **134**, 9741–9748.
- M. K. Kocik, O. O. Mykhaylyk and S. P. Armes, *Soft Matter*, 2014, **10**, 3984–3992.
- C. Gonzato, M. Semsarilar, E. R. Jones, F. Li, G. J. P. Krooshof, P. Wyman, O. O. Mykhaylyk, R. Tuinier and S. P. Armes, *J. Am. Chem. Soc.*, 2014, **136**, 11100–11106.
- V. J. Cunningham, L. P. D. Ratcliffe, A. Blanz, N. J. Warren, A. J. Smith, O. O. Mykhaylyk and S. P. Armes, *Polym. Chem.*, 2014, **5**, 6307–6317.
- J. S. Pedersen and M. C. Gerstenberg, *Macromolecules*, 1996, **29**, 1363–1365.
- J. S. Pedersen and P. Schurtenberger, *Macromolecules*, 1996, **29**, 7602–7612.
- J. S. Pedersen, *J. Appl. Cryst.*, 2000, **33**, 637–640.
- J. Ilavsky and P. R. Jemian, *J. Appl. Cryst.*, 2009, **42**, 347–353.
- M. J. Derry, L. A. Fielding, N. J. Warren, C. J. Mable, A. J. Smith, O. O. Mykhaylyk and S. P. Armes, *Chem. Sci.*, 2016, **7**, 5078–5090.
- T. Krouglov, W. H. Kraan, J. Plomp, M. T. Rekveldt and W. G. Bouwman, *J. Appl. Cryst.*, 2003, **36**, 816–819.
- T. Krouglov, W. G. Bouwman, J. Plomp, M. T. Rekveldt, G. J. Vroege, A. V. Petukhov and D. M. E. Thies-Weesie, *J. Appl. Cryst.*, 2003, **36**, 1417–1423.
- W. G. Bouwman, T. V. Krouglov, J. Plomp, S. V. Grigoriev, W. H. Kraan and M. T. Rekveldt, *Physica B: Condens. Matter*, 2004, **350**, 140–146.
- T. V. Krouglov, W. G. Bouwman, I. M. de Schepper and T. M. Rekveldt, *Physica B: Condens. Matter*, 2005, **356**, 218–222.
- A. L. Washington, X. Li, A. B. Schofield, K. Hong, M. R. Fitzsimmons, R. Dalglish and R. Pynn, *Soft Matter*, 2014, **10**, 3016–3026.
- S. R. Parnell, A. L. Washington, A. J. Parnell, A. Walsh, R. M. Dalglish, F. Li, W. A. Hamilton, S. Prevost, J. P. A. Fairclough and R. Pynn, *Soft Matter*, 2016, **12**, 4709–4714.
- J. Plomp, *Ph.D. thesis*, TU Delft, 2009.
- A. Guinier and G. Fournet, *Small-Angle Scattering of X-Rays*, John Wiley & Sons, New York, 1955.
- J. K. Percus and G. J. Yevick, *Phys. Rev.*, 1958, **110**, 1–13.
- A. Blanz, A. J. Ryan and S. P. Armes, *Macromolecules*, 2012, **45**, 5099–5107.